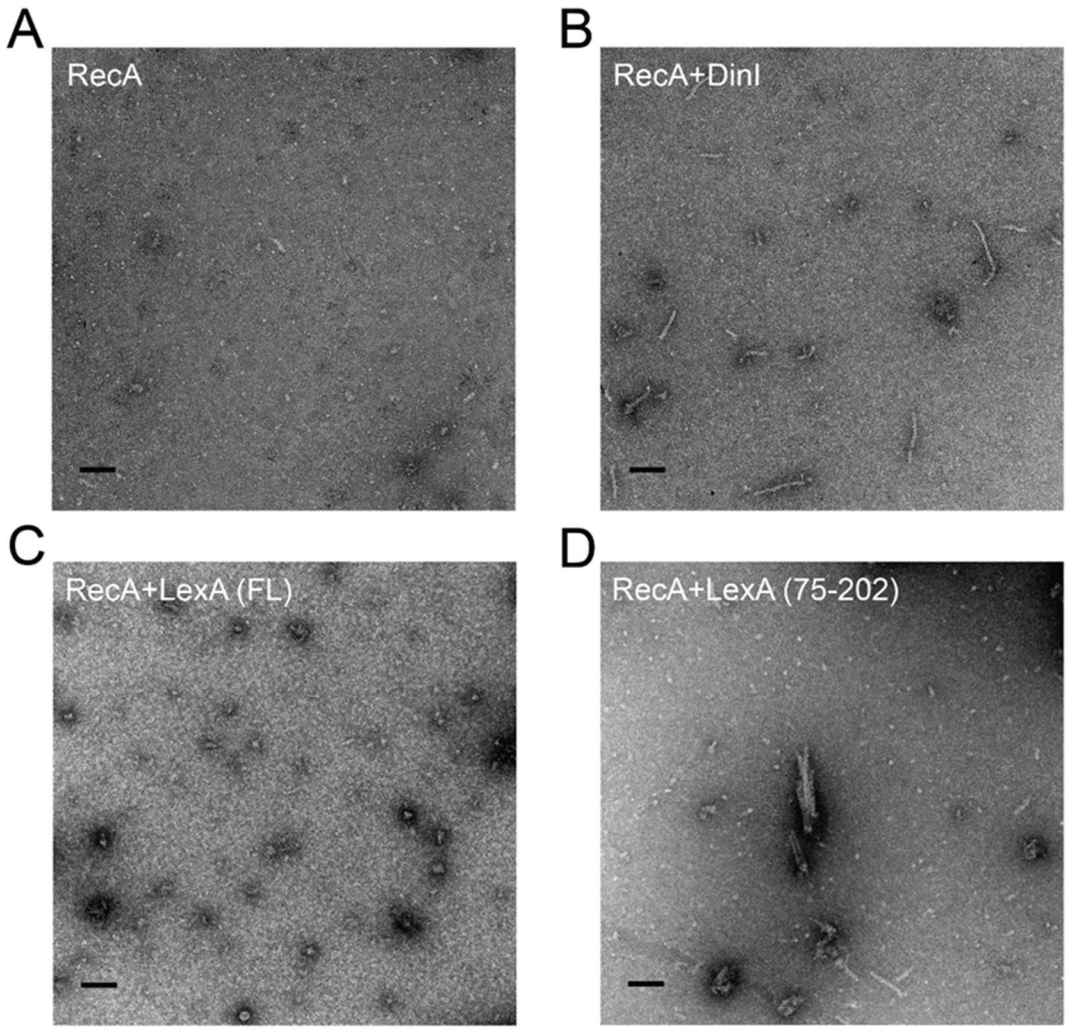

Fig. S1. Negative staining EM of RecA filaments formed with or without DinI, full-length LexA, and NTD truncated LexA.

(*A*) A representative EM photo of RecA filaments in the absence of DinI. The scale bar is 100 nm. Fifteen random fields were imaged with similar results.

(*B*) A representative EM photo of RecA filaments in the presence of DinI. The scale bar is 100 nm. Fifteen random fields were imaged with similar results.

(*C*) A representative EM photo of RecA filaments in the presence of full-length LexA (K156A). The scale bar is 100 nm. Fifteen random fields were imaged with similar results.

(*D*) A representative EM photo of RecA filaments in the presence of NTD truncated LexA (K156A). The scale bar is 100 nm. Fifteen random fields were imaged with similar results.

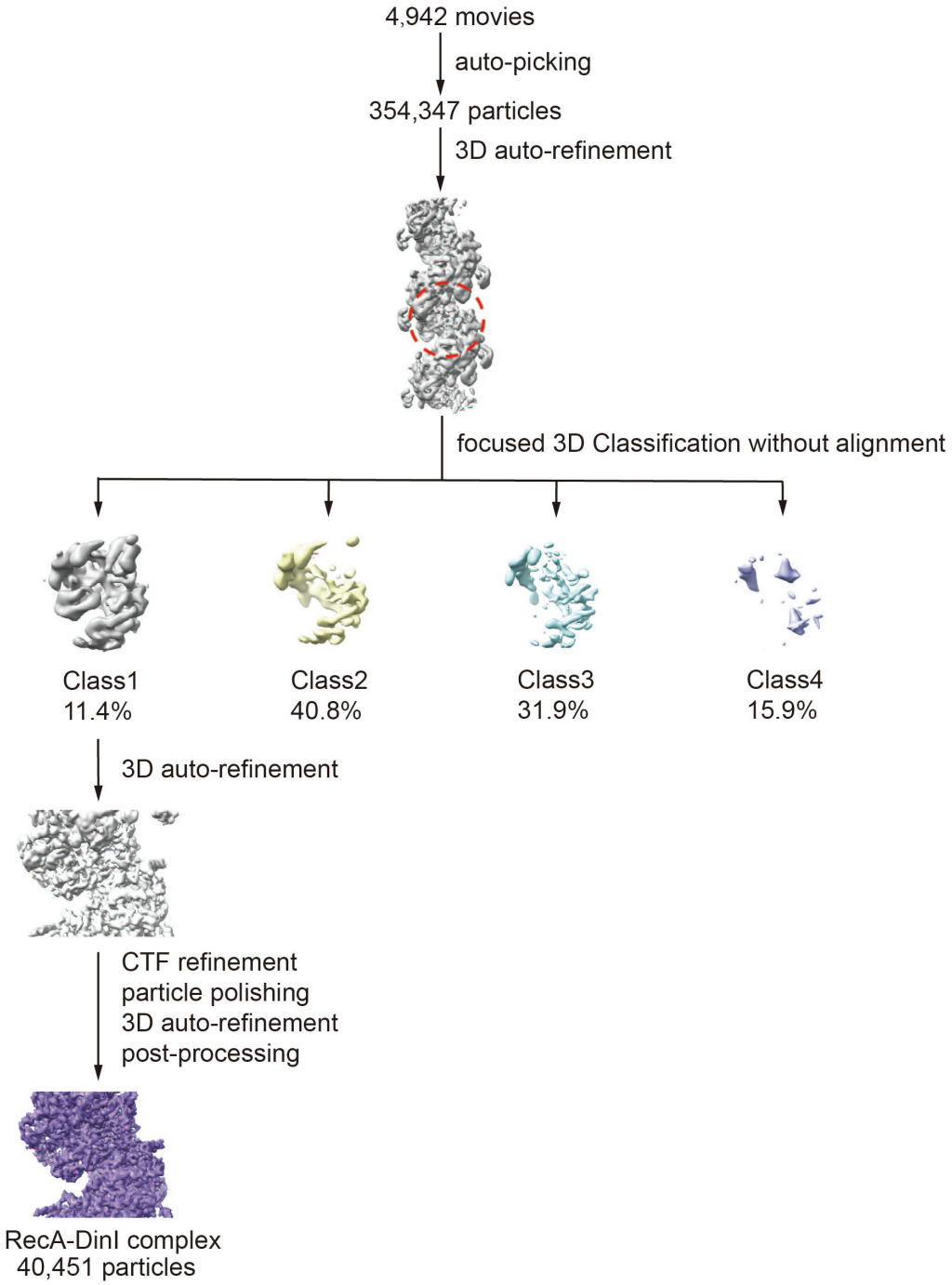

Fig. S2. Data processing pipeline for the dataset of RecA-DinI.

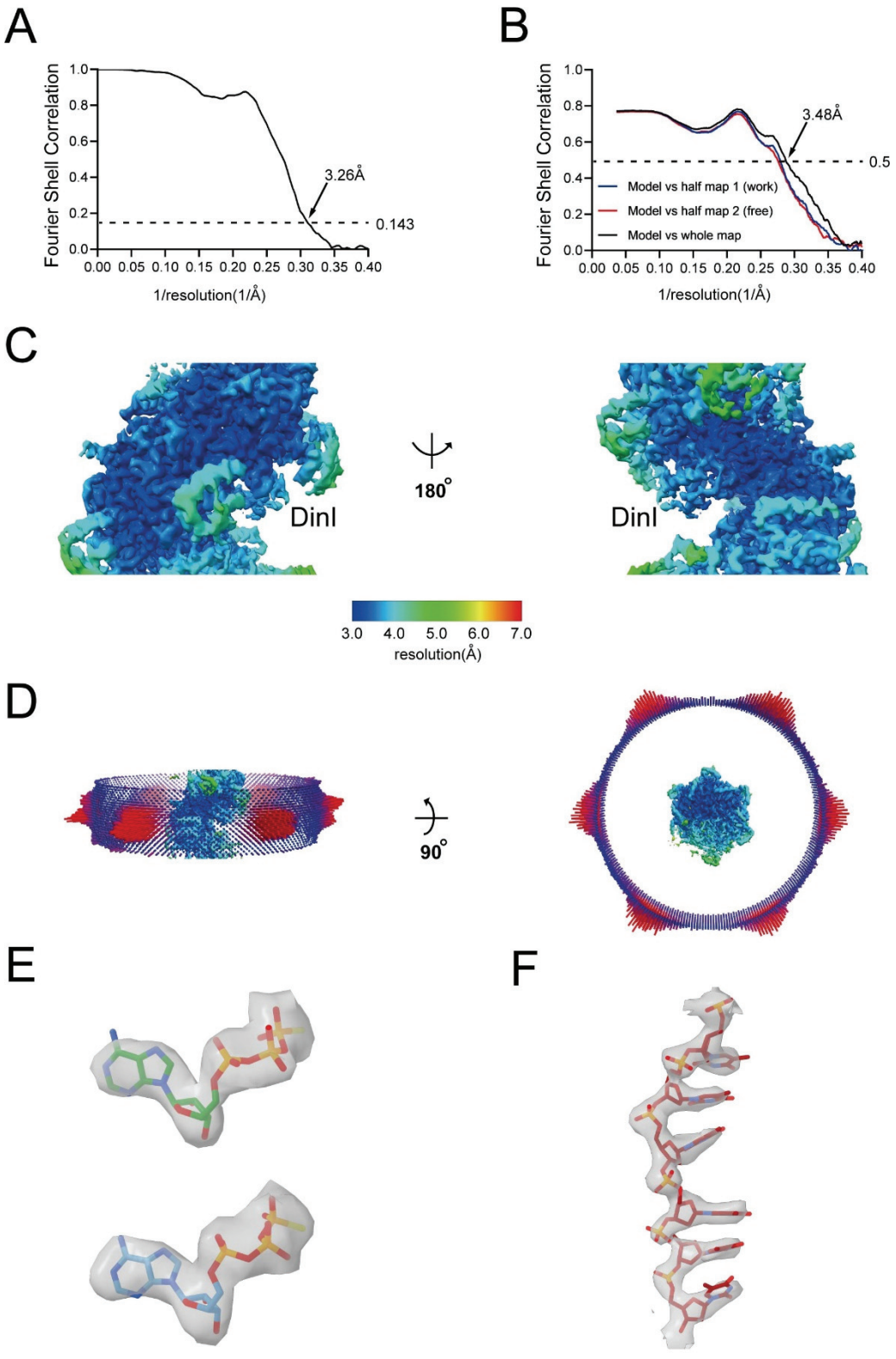

Fig. S3. Data validation for RecA-DinI.

(*A*) The gold-standard FSC of RecA-DinI. The gold-standard FSC is calculated by comparing the two independently determined half-maps from RELION. The dashed line represents the 0.143 FSC cutoff.

(*B*) FSC calculated between the model and the half map used for refinement (work), the other half map (free), and the full map.

(*C*) Cryo-EM density map colored by local resolution.

(*D*) Angular distribution of particle projections.

(*E*) The cryo-EM density map of two ATPγS molecules in each asymmetrical unit.

(*F*) The cryo-EM density of 6-nt oligo (dT) ssDNA in each asymmetrical unit.

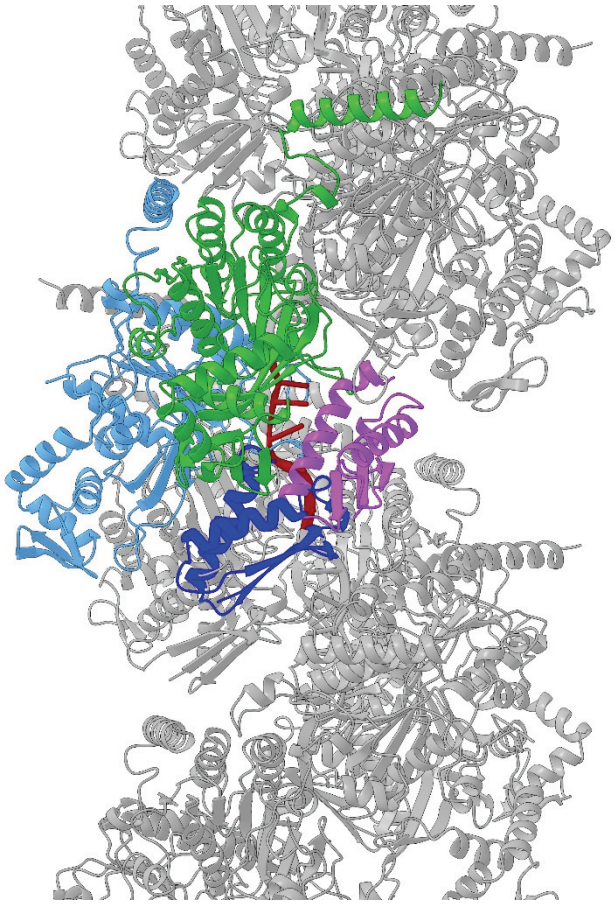

Fig. S4. The asymmetrical unit of RecA-DinI is composed of two RecA protomers and one DinI molecule.

The asymmetrical unit of RecA-DinI is colored as in Fig. 1*A*. If a second DinI molecule (dark blue) was modeled into the asymmetrical unit, there would be a steric clash between DinI molecules.

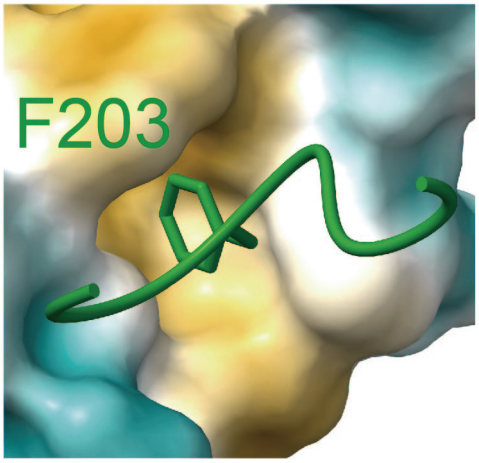

Fig. S5. F203 of RecA binds into a hydrophobic pocket in DinI.

DinI surface is colored according to hydrophobic potential. The surface coloring ranges from dark goldenrod for the most hydrophobic potentials to dark cyan for the most hydrophilic potentials.

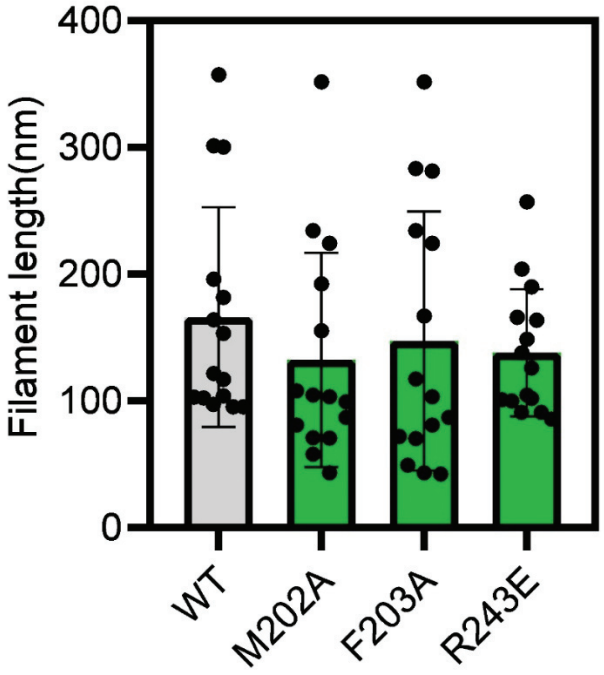

Fig. S6. Substitution of RecA residues doesn't affect RecA filament formation in the absence of DinI.

Fifteen random fields were imaged and the lengths of filaments longer than 40 nm were summed for each field.

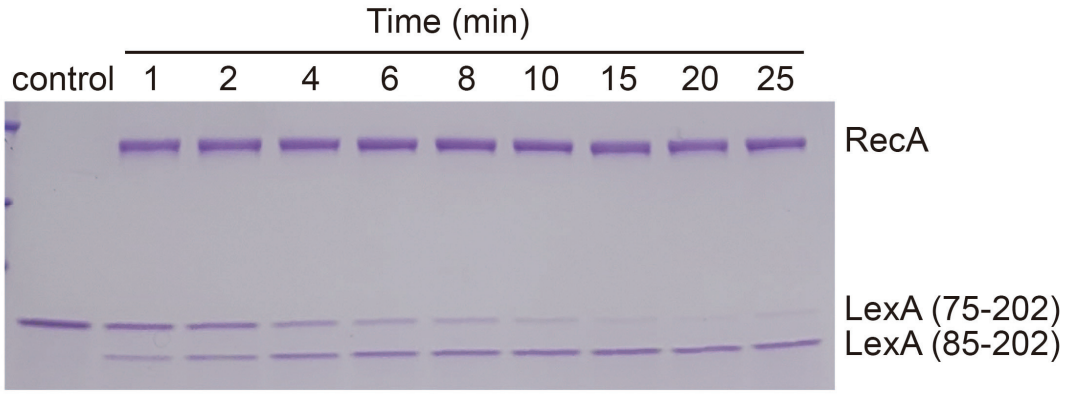

Fig. S7.LexA (residues 75 - 202) undergoes RecA mediated cleavage.

Experiments were repeated independently three times with similar results.

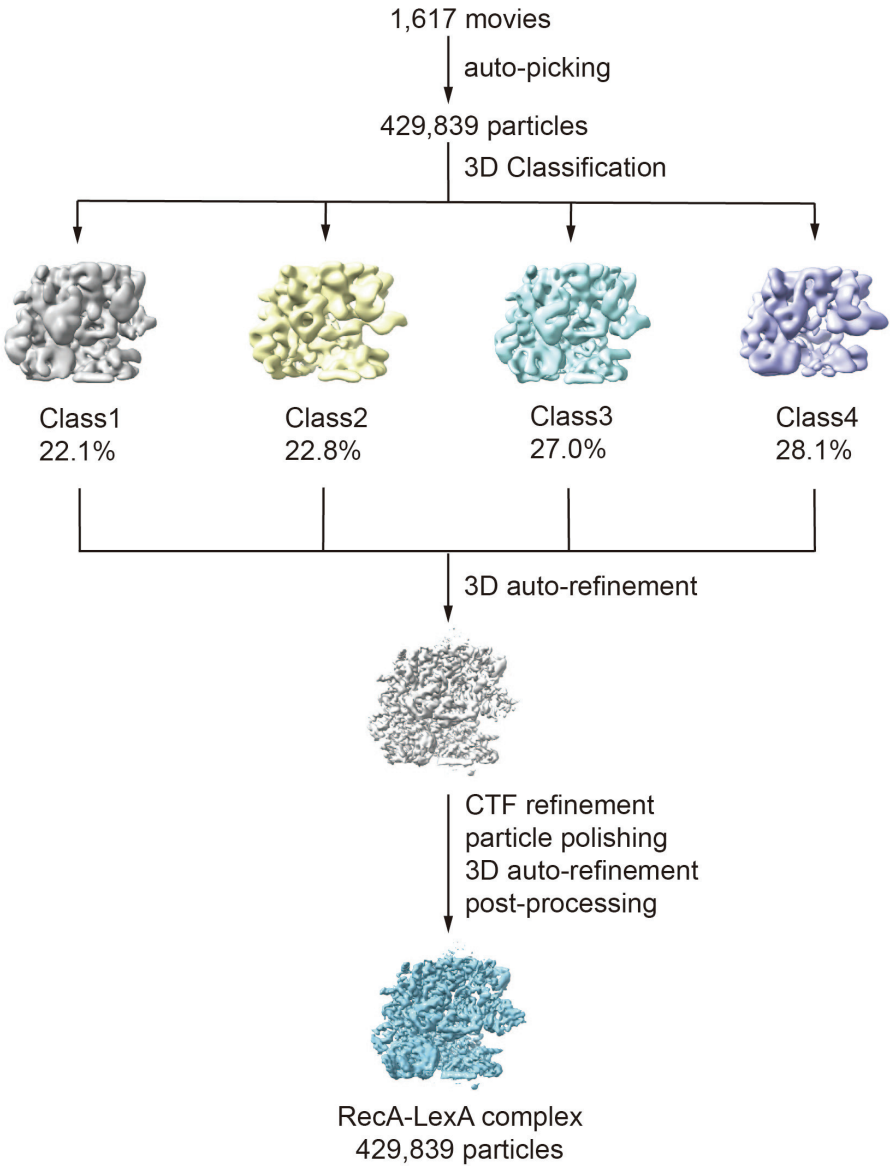

Fig. S8. Data processing pipeline for the dataset of RecA-LexA.

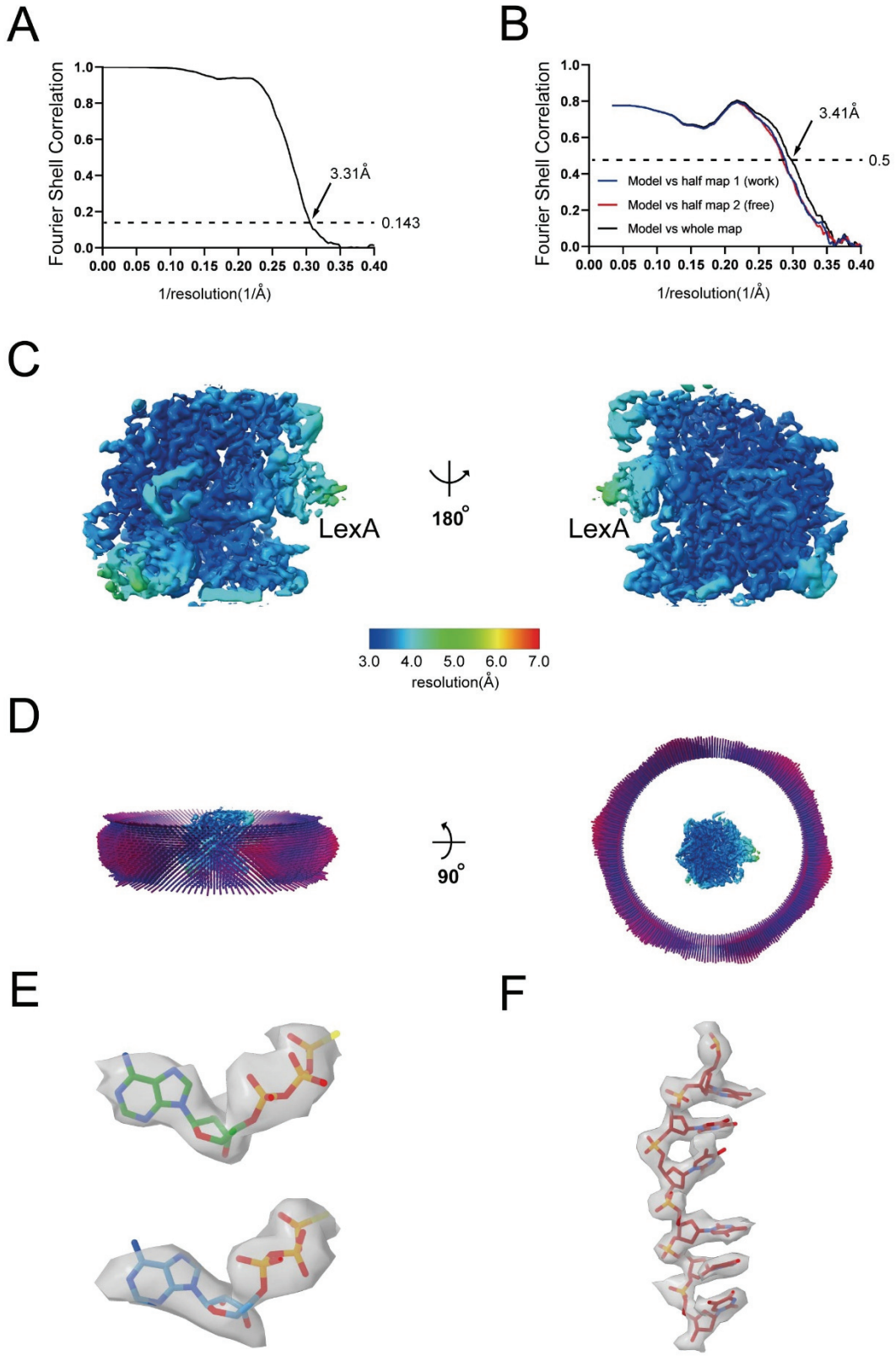

Fig. S9. Data validation for RecA-LexA.

(*A*) The gold-standard FSC of RecA-LexA. The gold-standard FSC is calculated by comparing the two independently determined half-maps from RELION. The dashed line represents the 0.143 FSC cutoff.

(*B*) FSC calculated between the model and the half map used for refinement (work), the other half map (free), and the full map.

(*C*) Cryo-EM density map colored by local resolution.

(*D*) Angular distribution of particle projections.

(*E*) The cryo-EM density map of two ATPγS molecules in each asymmetrical unit.

(*F*) The cryo-EM density of 6-nt oligo (dT) ssDNA in each asymmetrical unit.

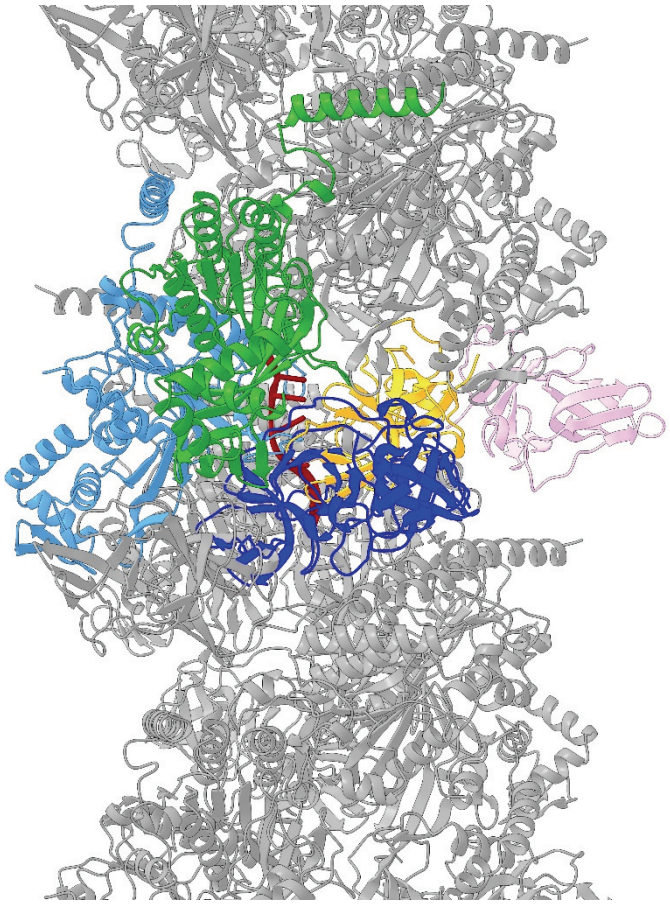

Fig. S10. The asymmetrical unit of RecA-LexA is composed of two RecA protomers and one LexA dimer.

The asymmetrical unit of RecA-LexA is colored as in Fig. 2*A*. If a second LexA dimer (dark blue) was modeled into the asymmetrical unit, there would be a steric clash between LexA dimers.

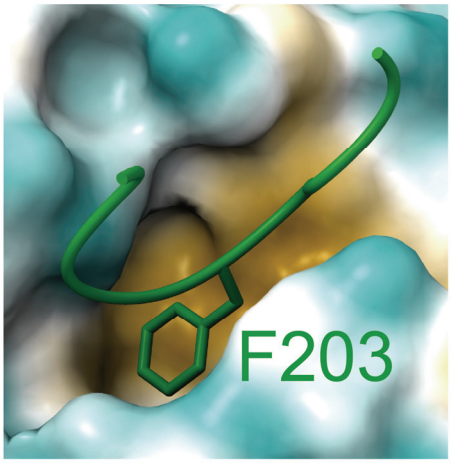

Fig. S11. F203 of RecA binds into a hydrophobic pocket in LexA[i].

LexA surface is colored according to hydrophobic potential. The surface coloring ranges from dark goldenrod for the most hydrophobic potentials to dark cyan for the most hydrophilic potentials.

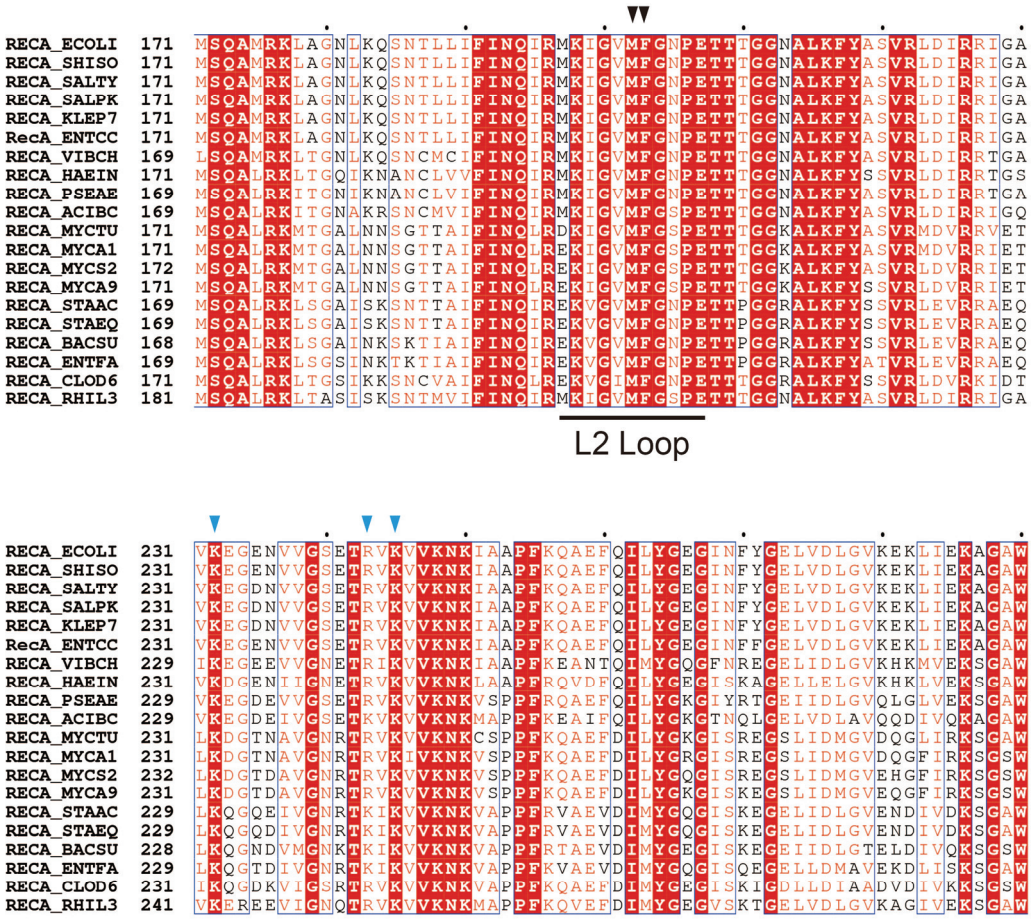

Fig. S12. Sequence alignment of RecA homologs.

The sequences were aligned using Clustal Omega and the figure was prepared using ESPript 3.0. Black and cyan triangles indicate residues making hydrophobic interactions and electrostatic interactions, respectively. Species are as follows: *Escherichia coli* (ECOLI), *Shigella sonnei* (SHISO), *Salmonella typhimurium* (SALTY), *Salmonella paratyphi A* (SALPK), *Klebsiella pneumoniae* (KLEP7), *Enterococcus cloacae* (ENTCC), *Vibrio cholerae* (VIBCH), *Haemophilus influenzae* (HAEIN), *Pseudomonas aeruginosa* (PSEAE), *Acinetobacter baumannii* (ACIBC), *Mycobacterium tuberculosis* (MYCTU), *Mycobacterium avium* (MYCA1), *Mycolicibacterium smegmatis* (MYCS2), *Mycobacterium abscessus* (MYCA9), *Staphylococcus aureus* (STAAC), *Staphylococcus epidermidis* (STAEQ), *Bacillus subtilis* (BACSU), *Enterococcus faecalis* (ENTFA), *Clostridioides difficile* (CLOD6), *Rhizobium leguminosarum* (RHIL3).

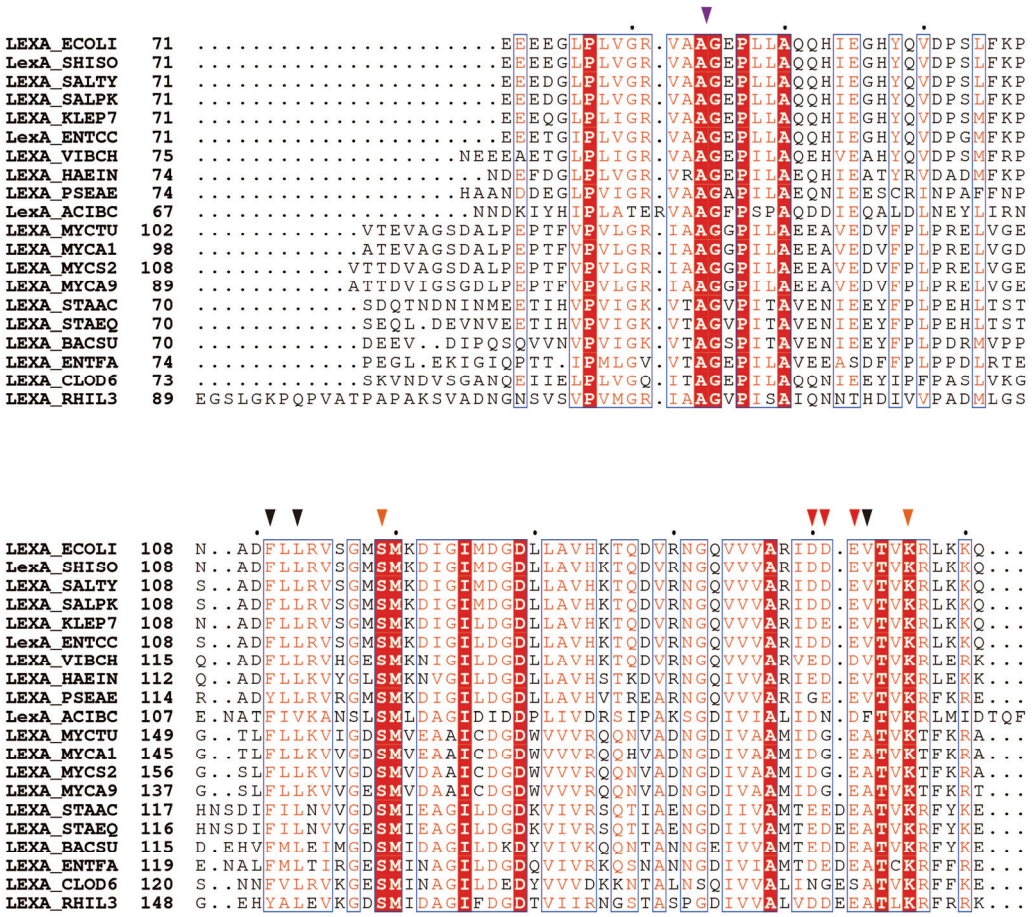

Fig. S13. Sequence alignment of LexA homologs.

The sequences were aligned using Clustal Omega and the figure was prepared using ESPript 3.0. Black and red triangles indicate residues making hydrophobic interactions and electrostatic interactions, respectively. Purple triangle, the cleavage peptide bond; orange triangles, the Ser-Lys catalytic dyad. Species are as follows: *Escherichia coli* (ECOLI), *Shigella sonnei* (SHISO), *Salmonella typhimurium* (SALTY), *Salmonella paratyphi A* (SALPK), *Klebsiella pneumoniae* (KLEP7), *Enterococcus cloacae* (ENTCC), *Vibrio cholerae* (VIBCH), *Haemophilus influenzae* (HAEIN), *Pseudomonas aeruginosa* (PSEAE), *Acinetobacter baumannii* (ACIBC), *Mycobacterium tuberculosis* (MYCTU), *Mycobacterium avium* (MYCA1), *Mycolicibacterium smegmatis* (MYCS2), *Mycobacterium abscessus* (MYCA9), *Staphylococcus aureus* (STAAC), *Staphylococcus epidermidis* (STAEQ), *Bacillus subtilis* (BACSU), *Enterococcus faecalis* (ENTFA), *Clostridioides difficile* (CLOD6), *Rhizobium leguminosarum* (RHIL3).

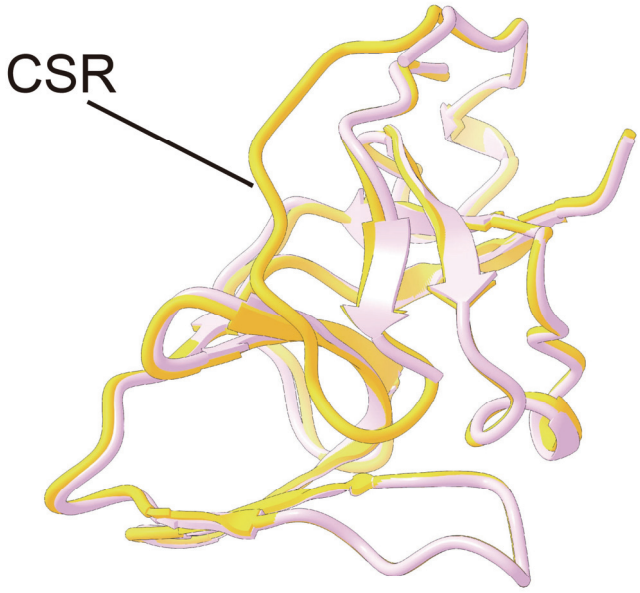

Fig. S14. Structural comparison of LexA^{i} and LexA^{o} shows that the CSR of LexA^{o} is disordered.

Yellow, LexA^{i}; pink, LexA^{o}.

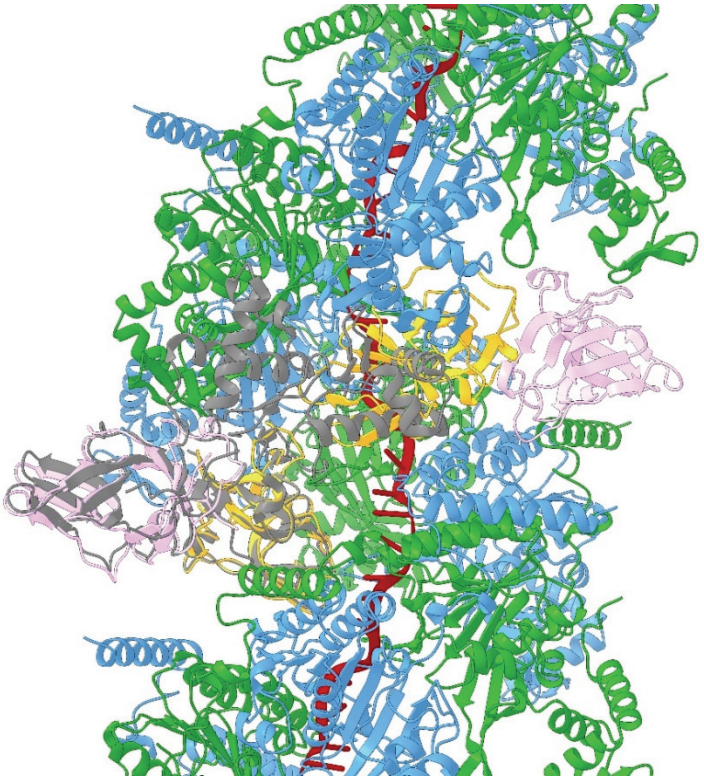

Fig. S15. Superposition of RecA-LexA and full-length LexA structures shows steric clashes between the NTD and CTD of neighboring LexA molecules.

Yellow and pink, LexA in RecA-LexA; gray, crystal structure of full-length LexA (PDB 3JSP).

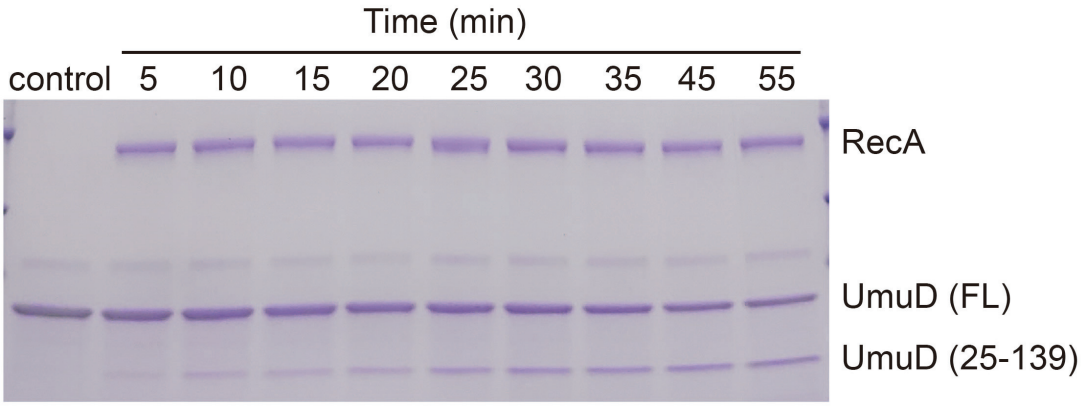

Fig. S16. UmuD undergoes RecA mediated cleavage.

Experiments were repeated independently three times with similar results.

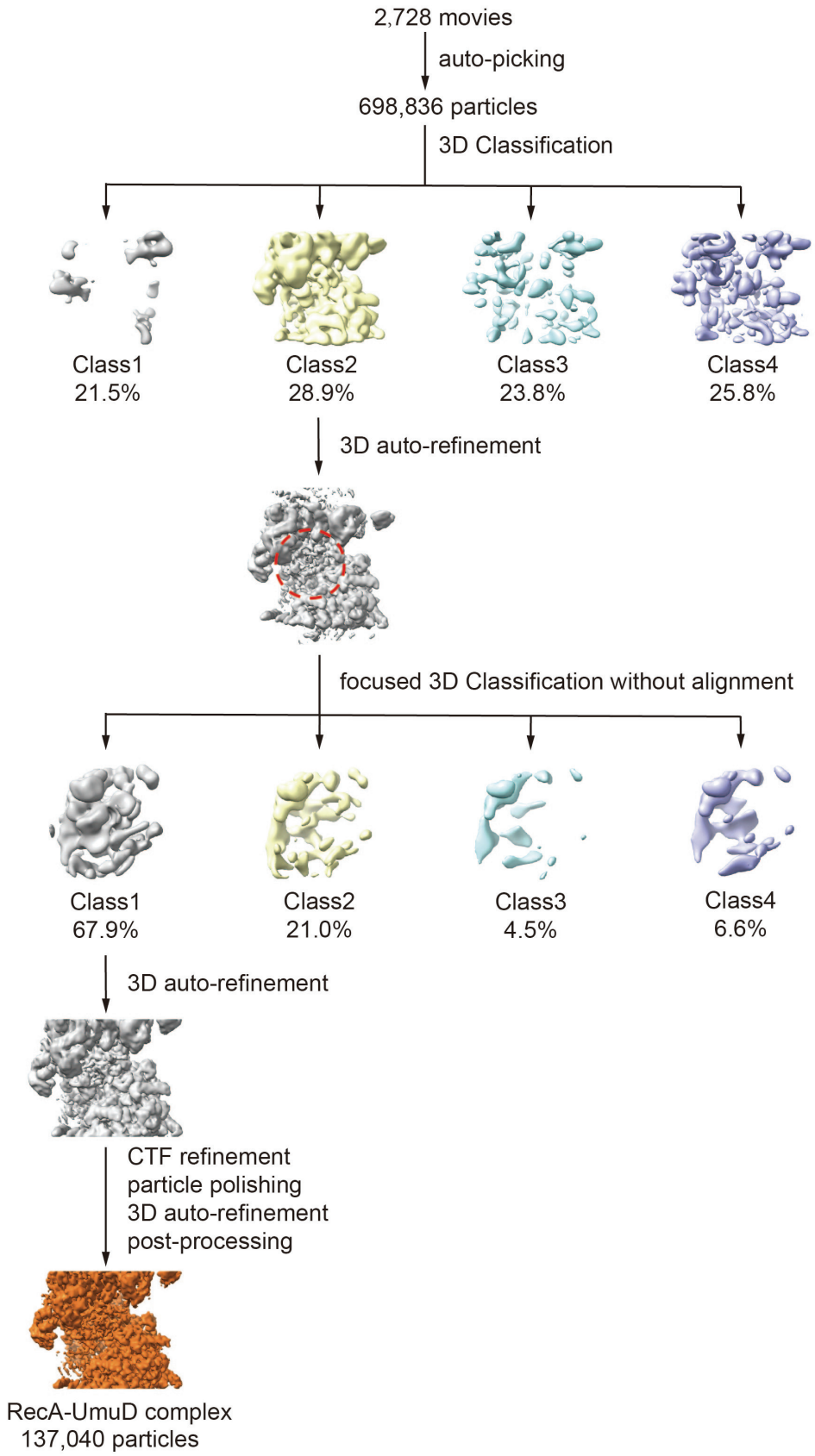

Fig. S17. Data processing pipeline for the dataset of RecA-UmuD.

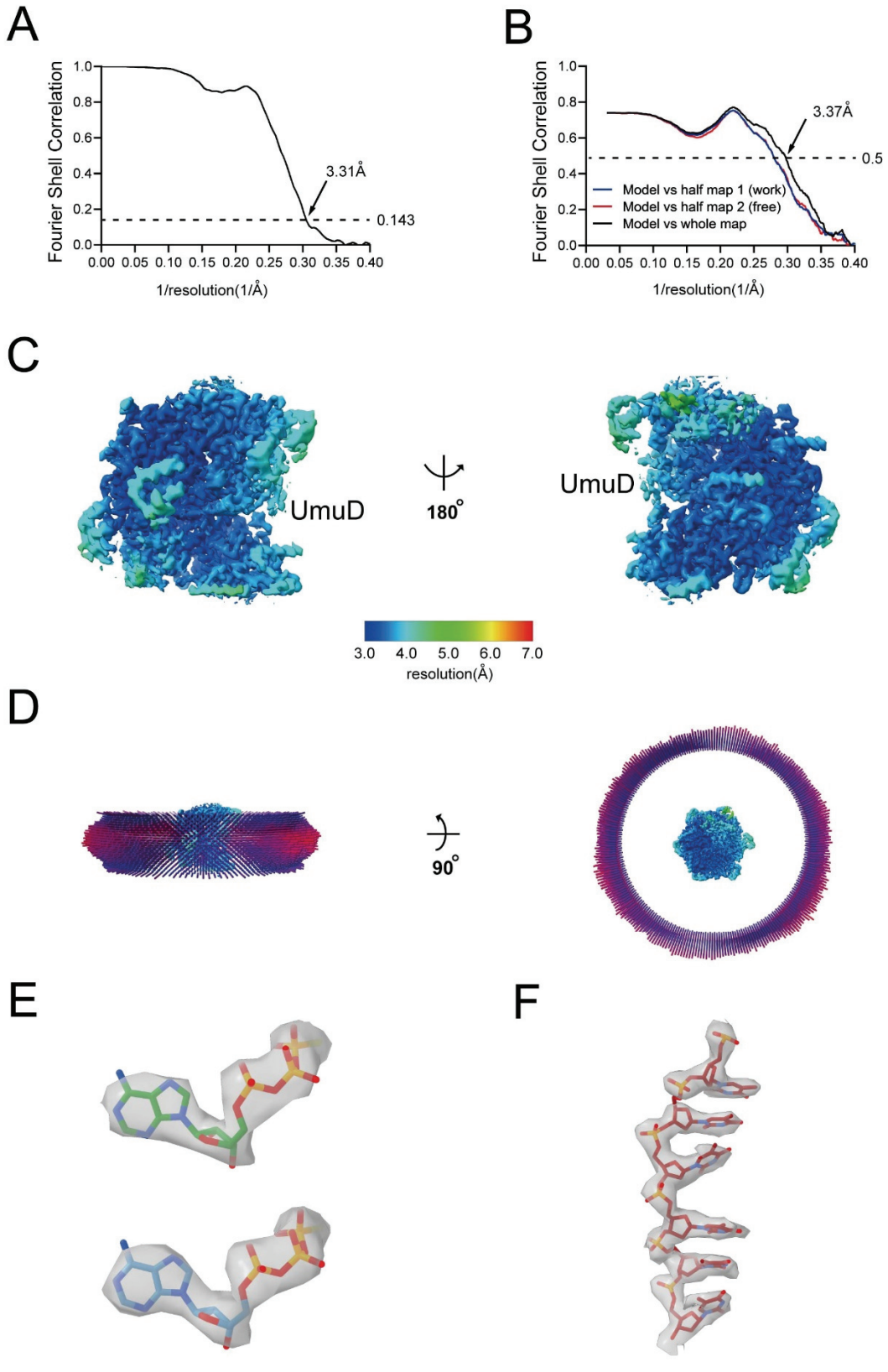

Fig. S18. Data validation for RecA-UmuD.

(*A*) The gold-standard FSC of RecA-UmuD. The gold-standard FSC is calculated by comparing the two independently determined half-maps from RELION. The dashed line represents the 0.143 FSC cutoff.

(*B*) FSC calculated between the model and the half map used for refinement (work), the other half map (free), and the full map.

(*C*) Cryo-EM density map colored by local resolution.

(*D*) Angular distribution of particle projections.

(*E*) The cryo-EM density map of two ATPγS molecules in each asymmetrical unit.

(*F*) The cryo-EM density of 6-nt oligo (dT) ssDNA in each asymmetrical unit.

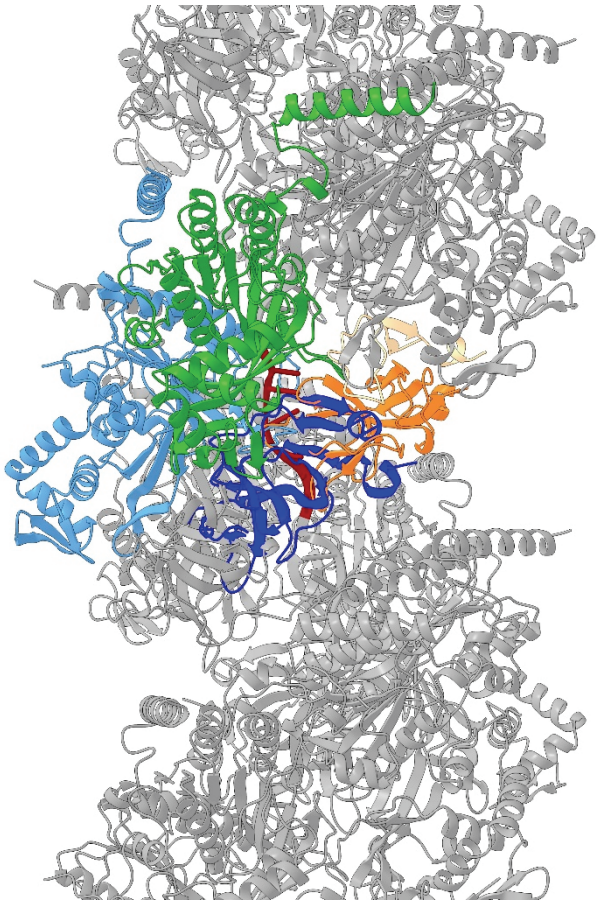

Fig. S19. The asymmetrical unit of RecA-UmuD is composed of two RecA protomers and one UmuD dimer.

The asymmetrical unit of RecA-UmuD is colored as in Fig. 3*A*. If a second UmuD dimer (dark blue) was modeled into the asymmetrical unit, there would be a steric clash between UmuD dimers.

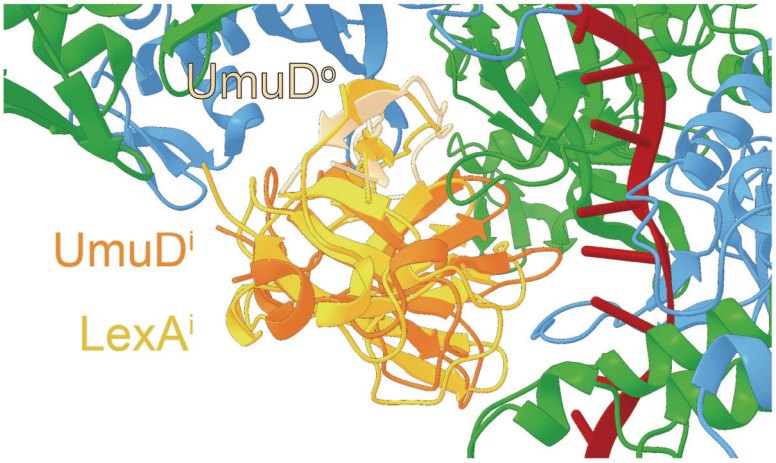

Fig. S20. Structural comparison of RecA-LexA and RecA-UmuD.

LexA^{o} and part of UmuD^{o} is omitted for clarity.

Fig. S21. F203 of RecA binds into a hydrophobic pocket in UmuD.

UmuD surface is colored according to hydrophobic potential. The surface coloring ranges from dark goldenrod for the most hydrophobic potentials to dark cyan for the most hydrophilic potentials.

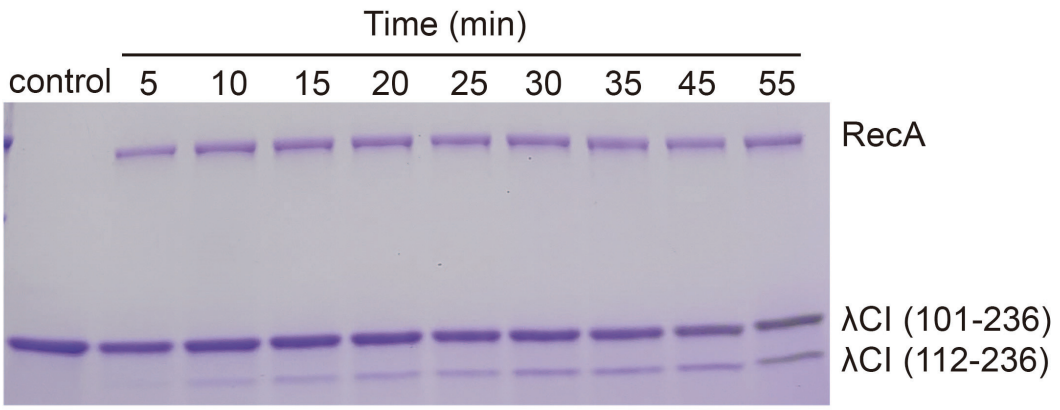

Fig. S22. λCI (residues 101 - 236) undergoes RecA mediated cleavage.

Experiments were repeated independently three times with similar results.

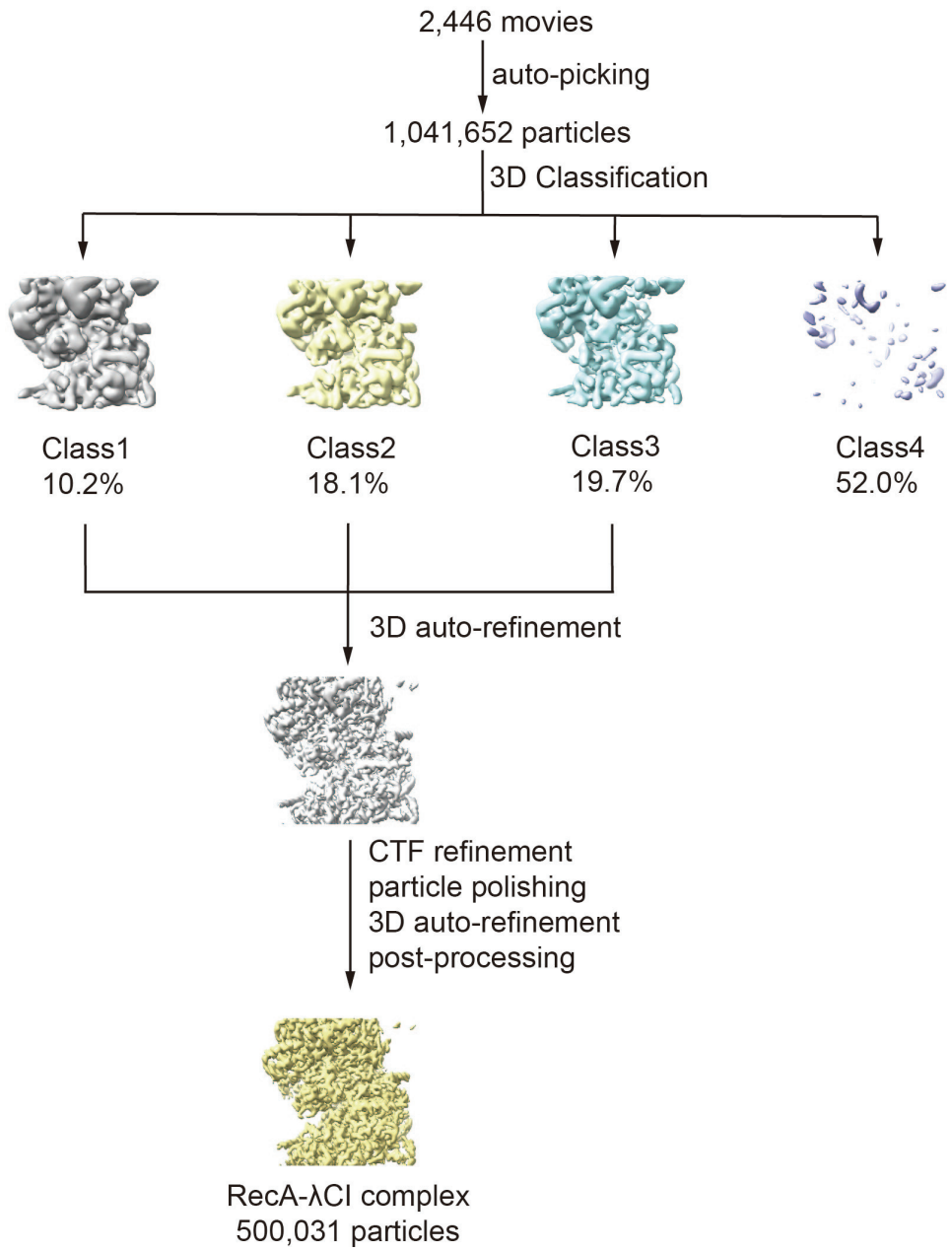

Fig. S23. Data processing pipeline for the dataset of RecA-λCI.

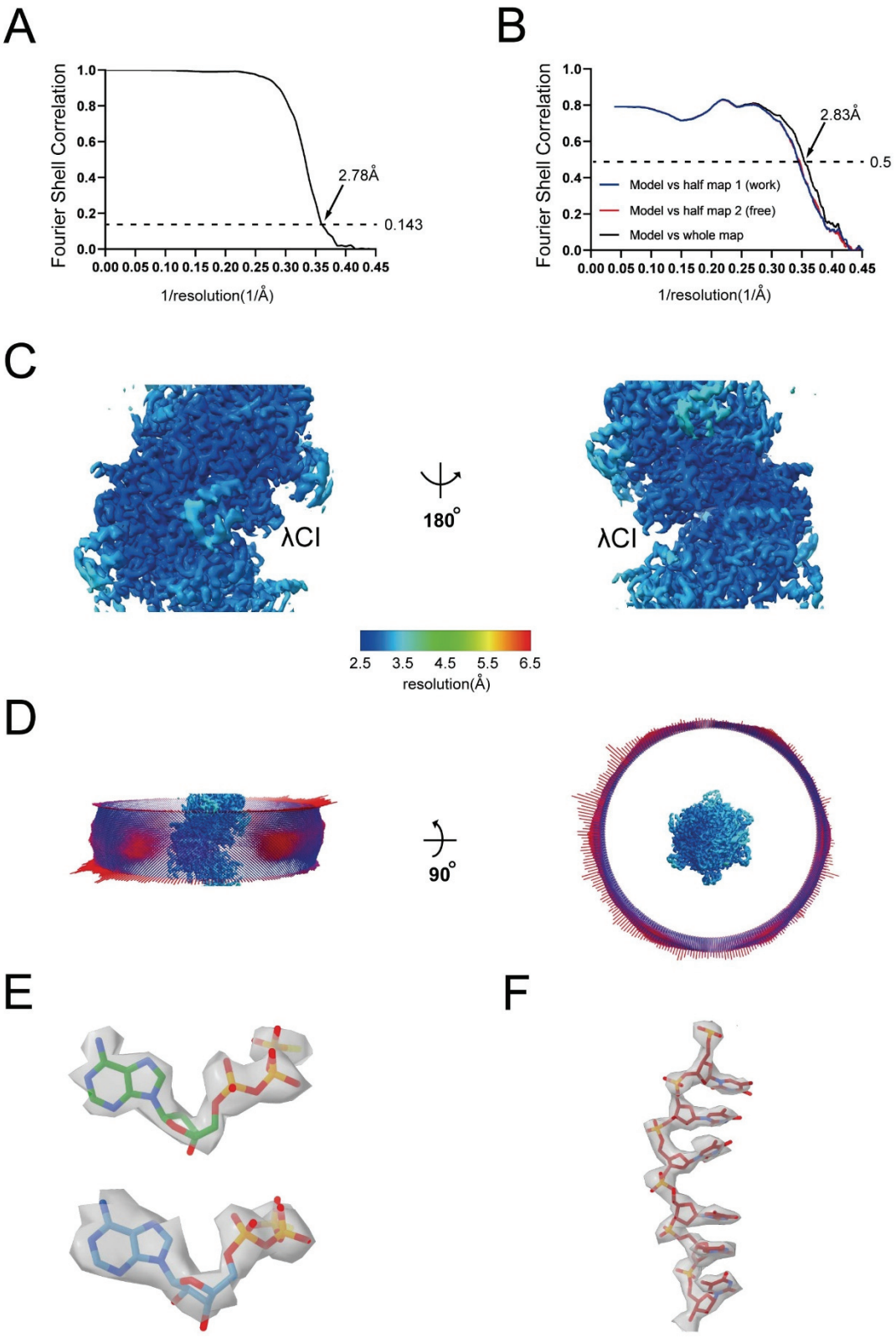

Fig. S24. Data validation for RecA-λCI.

(*A*) The gold-standard FSC of RecA-λCI. The gold-standard FSC is calculated by comparing the two independently determined half-maps from RELION. The dashed line represents the 0.143 FSC cutoff.

(*B*) FSC calculated between the model and the half map used for refinement (work), the other half map (free), and the full map.

(*C*) Cryo-EM density map colored by local resolution.

(*D*) Angular distribution of particle projections.

(*E*) The cryo-EM density map of two ATPγS molecules in each asymmetrical unit.

(*F*) The cryo-EM density of 6-nt oligo (dT) ssDNA in each asymmetrical unit.

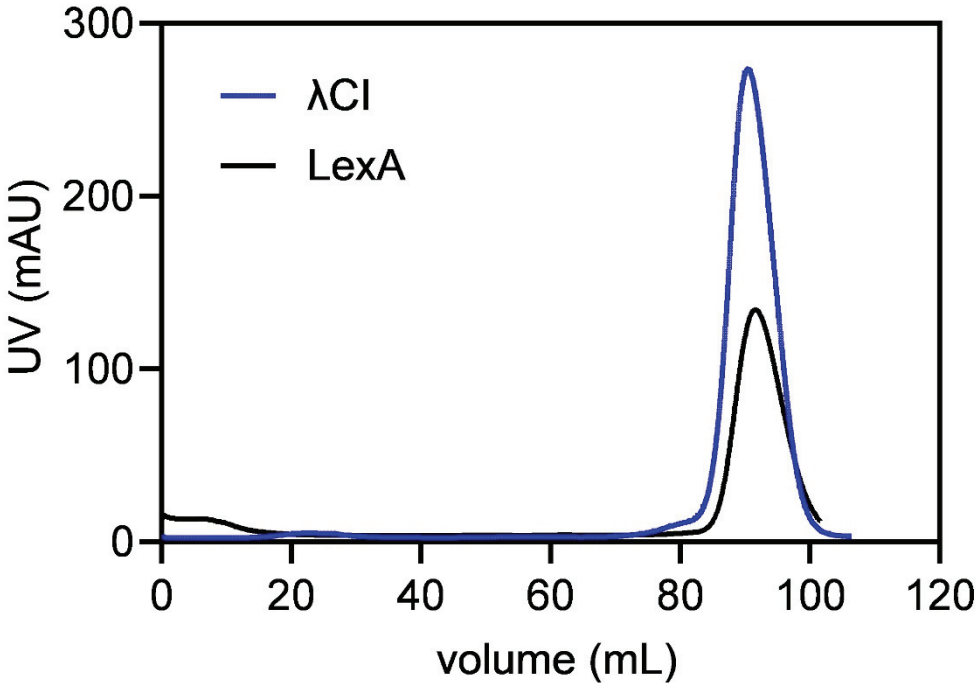

Fig. S25. The elution volume of NTD truncated λCI is the same as NTD truncated LexA in gel filtration experiments.

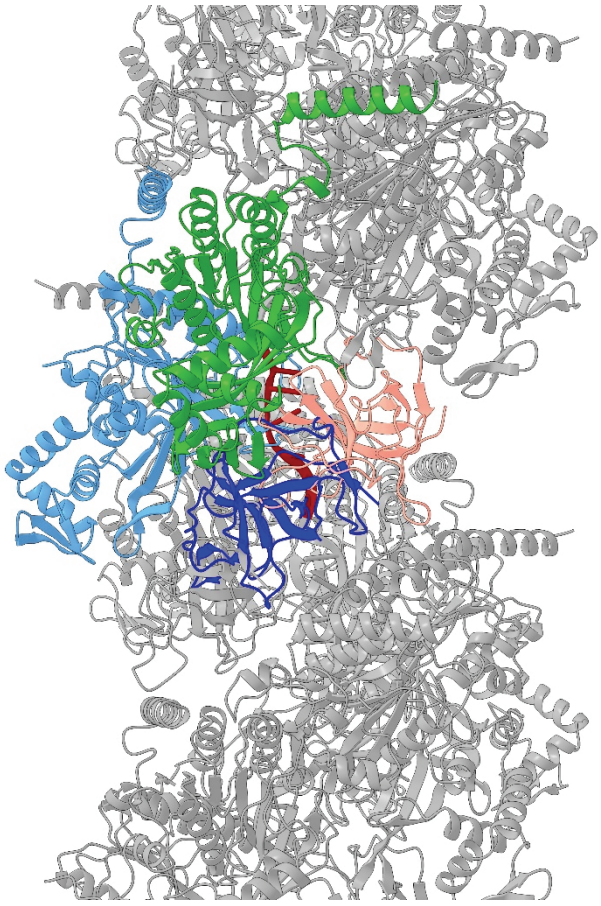

Fig. S26. The asymmetrical unit of RecA-λCI is composed of two RecA protomers and one λCI molecule.

The asymmetrical unit of RecA-λCI is colored as in Fig. 4*A*. If a second λCI molecule (dark blue) was modeled into the asymmetrical unit, there would be a steric clash between λCI molecules.

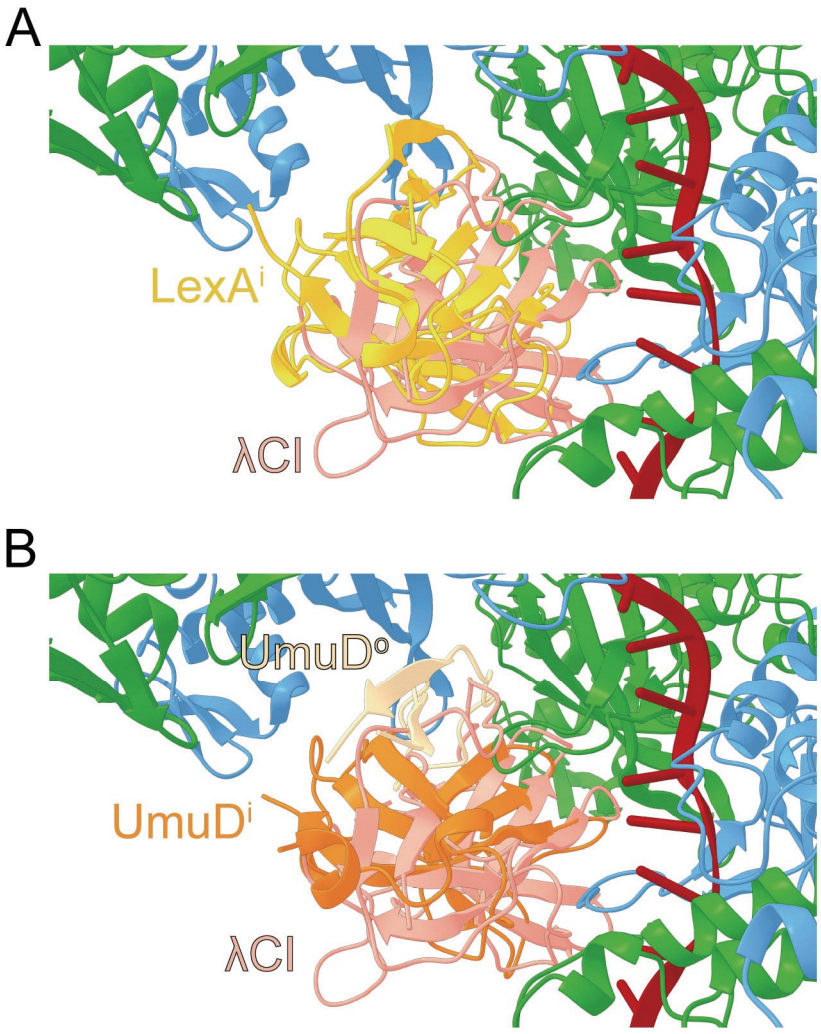

Fig. S27. Structural comparison of RecA-λCI, RecA-LexA, and RecA-UmuD shows that the orientation of λCI is different from LexA and UmuD.

(*A*) Structural comparison of RecA-λCI and RecA-LexA. LexA^{o} is omitted for clarity.

(*B*) Structural comparison of RecA-λCI and RecA-UmuD. Part of UmuD^{o} is omitted for clarity.

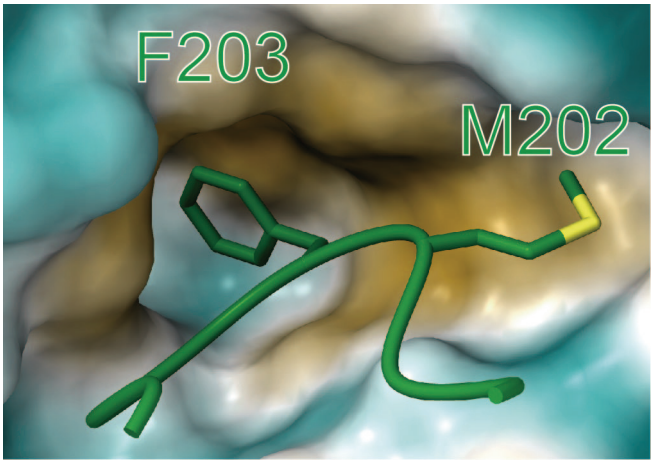

Fig. S28. M202 and F203 of RecA bind into a hydrophobic pocket in λCI.

λCI surface is colored according to hydrophobic potential. The surface coloring ranges from dark goldenrod for the most hydrophobic potentials to dark cyan for the most hydrophilic potentials.

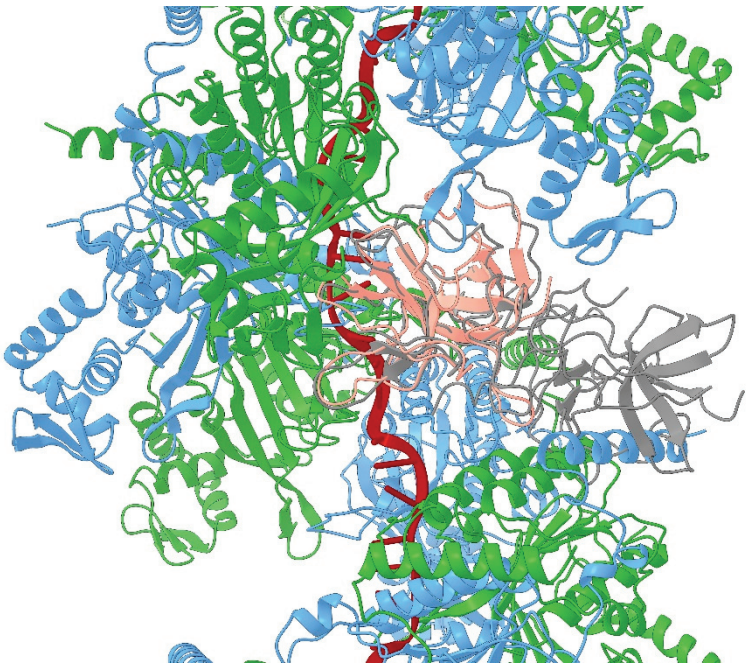

Fig. S29. Superposition of RecA-λCI and λCI dimer structures shows steric clashes between RecA and the outside λCI protomer.

Salmon, λCI in RecA-λCI; gray, crystal structure of λCI dimer (PDB 3BDN, NTD is omitted for clarity).

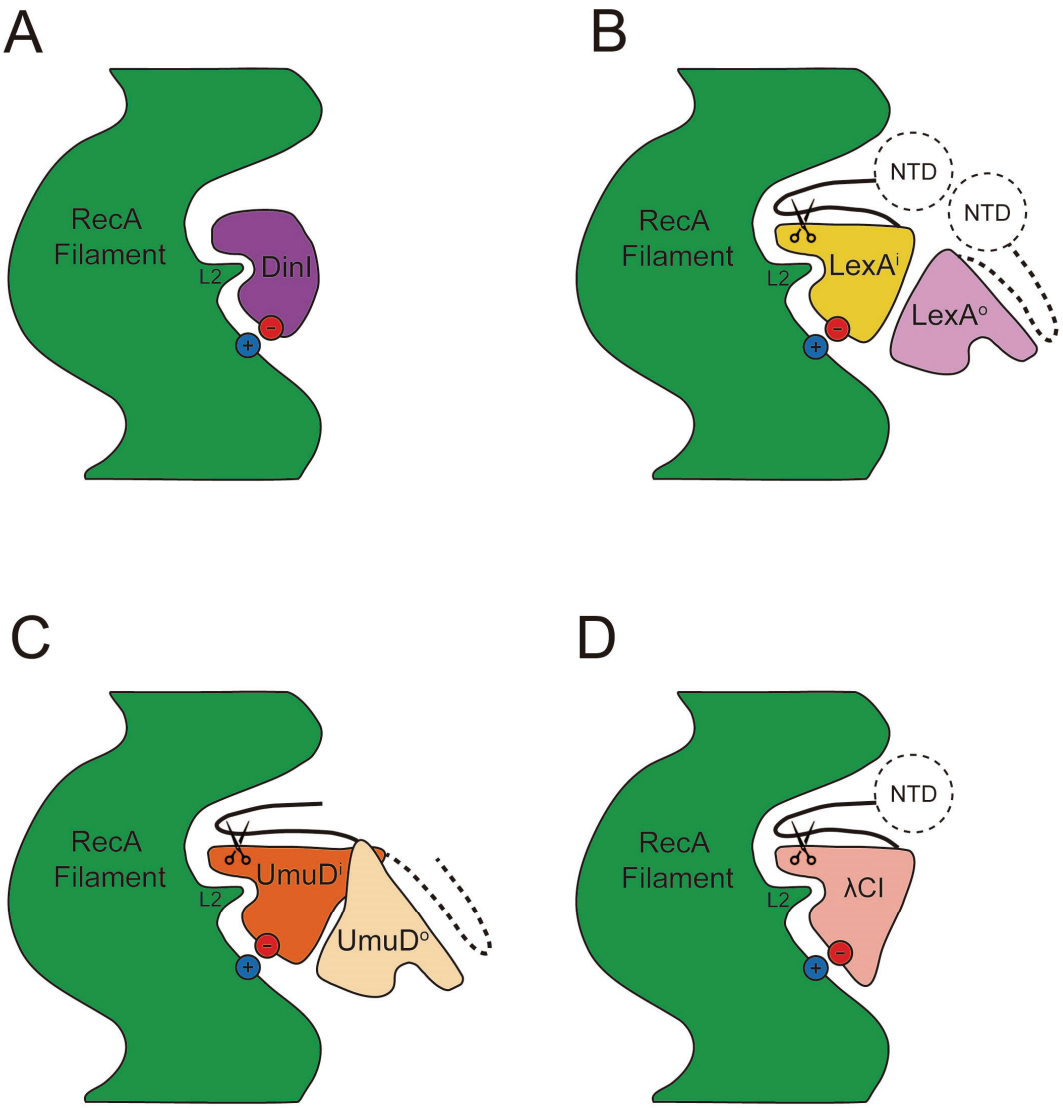

Fig. S30. The schematic diagrams of RecA-DinI (*A*), RecA-LexA (*B*), RecA-UmuD (*C*), and RecA-λCI (*D*).

Table S1. Cryo-EM data collection and refinement statistics.

	RecA-DinI	RecA-LexA	RecA-UmuD	RecA-λCI
Data collection and processing				
Microscope	Titan Krios	Titan Krios	Titan Krios	Titan Krios
Voltage (kv)	300	300	300	300
Detector	Falcon 4	Falcon 4	Falcon 4	Falcon 4
Electron exposure (e/Å^2)	62	52	52	50
Defocus range (μm)	1.0 - 2.0	1.0 - 2.0	0.8 - 1.7	0.8 - 1.7
Data collection mode	Counting	Counting	Counting	Counting
Physical pixel size (Å/pixel)	0.93	1.19	1.19	1.19
Symmetry imposed	Helical	Helical	Helical	Helical
Twist (°)	118.0	118.6	118.3	118.1
Rise (Å)	31.5	31.5	31.6	31.5
Initial particle images	354,347	429,839	698,836	1,041,652
Final particle images	40,451	429,839	137,040	500,031
Map resolution (Å)[a]	3.3	3.3	3.3	2.8
Refinement				
Root-mean-square deviation				
Bond lengths (Å)	0.003	0.003	0.003	0.003
Bond angles (°)	0.631	0.564	0.794	0.497
Molprobity statistics				
Clashscore	11.67	9.68	8.99	8.36
Rotamer outliers (%)	0.34	0.41	0.31	1.89
Cβ outliers (%)	0	0	0	0
Ramachandran plot				
Favored (%)	97	97	98	98
Outliers (%)	0	0	0	0.25

[a]Gold-standard FSC 0.143 cutoff criteria.

Table S2. RecA-DinI interface surface area (Å^2) statistics.

	DinI
RecA^2	238
RecA^3	370
RecA^4	231
RecA^5	125
RecA^6	19
Sum	983

Table S3. RecA-LexA interface surface area (Å^2) statistics.

	LexA^i	LexA^o
RecA^1	58	246
RecA^2	339	0
RecA^3	480	0
RecA^4	251	0
RecA^5	89	0
RecA^6	77	0
Sum	1294	246

Table S4. RecA-UmuD interface surface area (Å^2) statistics.

	UmuD^i	UmuD^o
RecA^1	0	51
RecA^2	21	502
RecA^3	439	302
RecA^4	216	0
RecA^5	28	0
RecA^6	8	0
Sum	712	855

Table S5. RecA-λCI interface surface area (Å^2) statistics.

	λCI
RecA^2	274
RecA^3	846
RecA^4	360
RecA^5	192
RecA^6	86
RecA^8	45
Sum	1803